

# Universal Feature in Optical Control of a $p$ -wave Feshbach Resonance

Peng Peng,<sup>1,2,\*</sup> Ren Zhang,<sup>3,4,\*</sup> Lianghui Huang,<sup>1,2,†</sup> Donghao Li,<sup>1,2</sup> Zengming Meng,<sup>1,2</sup> Pengjun Wang,<sup>1,2</sup> Hui Zhai,<sup>4,5</sup> Peng Zhang,<sup>6,7</sup> and Jing Zhang<sup>1,8,‡</sup>

<sup>1</sup>State Key Laboratory of Quantum Optics and Quantum Optics Devices,  
Institute of Opto-Electronics, Shanxi University, Taiyuan 030006, P.R.China

<sup>2</sup>Collaborative Innovation Center of Extreme Optics, Shanxi University, Taiyuan 030006, P.R.China

<sup>3</sup>Department of Applied Physics, Xi'an Jiaotong University, Shanxi, 710049, China

<sup>4</sup>Institute for Advanced Study, Tsinghua University, Beijing, 100084, China

<sup>5</sup>Collaborative Innovation Center of Quantum Matter, Beijing, 100084, China

<sup>6</sup>Department of Physics, Renmin University of China, Beijing, 100872, China

<sup>7</sup>Beijing Computational Science Research Center, Beijing, 100084, China

<sup>8</sup>Synergetic Innovation Center of Quantum Information and Quantum Physics,  
University of Science and Technology of China, Hefei, Anhui 230026, P. R. China

(Dated: June 19, 2022)

In this Letter we report the experimental results on optical control of a  $p$ -wave Feshbach resonance, by utilizing a laser driven bound-to-bound transition to shift the energy of closed channel molecule. The magnetic field location for  $p$ -wave resonance as a function of laser detuning can be captured by a simple formula with essentially one parameter, which describes how sensitive the resonance depends on the laser detuning. The key result of this work is to demonstrate, both experimentally and theoretically, that the ratio between this parameter for  $m = 0$  resonance and that for  $m = \pm 1$  resonance, to large extent, is universal. We also show that this optical control can create intriguing situations where interesting few- and many-body physics can occurs, such as a  $p$ -wave resonance overlapping with an  $s$ -wave resonance or three  $p$ -wave resonances being degenerate.

The capability of controlling the interaction strength between atoms has led to tremendous progresses in the field of ultracold atomic gases. Magnetic-field-induced Feshbach resonance is one of such powerful tools and has been widely used in studying strongly correlated degenerate atomic gases [1]. Another technique for tuning interatomic interactions is the optical Feshbach resonance, in which a pair of atoms in the scattering states are coupled to an excited molecular state by a near photoassociation resonance laser field [2]. The optical Feshbach resonance offers a more flexible spatial and temporal control of interaction, since the laser intensity can vary on short length and time scales [3, 4]. However, it also suffers from rapid losses of atoms due to the light-induced inelastic collisions between atoms.

Recently, an alternative method of optical control has been implemented to avoid the problem of atom losses, in which the optical control is combined with the magnetic Feshbach resonance [5–14]. The key idea is that, instead of coupling atoms in scattering states to a bound state, the laser induces a bound-to-bound transition between the closed channel molecule responsible for a magnetic Feshbach resonance and an excited molecular state. In this way, the laser can shift the energy of closed channel molecule, and thus moves the location of the magnetic Feshbach resonance. This method has been recently demonstrated in both ultracold Bose [6, 8, 11] and Fermi gases [10, 12]. It has been shown that the atom loss rate can be reduced by an order of magnitude, while the advantage of high resolution of spatial and temporal control is still maintained. To distinguish this method from the conventional optical Feshbach resonance, we shall refer

to it as the optical control of a magnetic Feshbach resonance.

$p$ -wave interaction plays a crucial role in many quantum many-body systems [15–20], especially in the realization of topological superfluids [21–23]. Thus, the intensively experimental efforts have been made on  $p$ -wave Feshbach resonance in the last decade [24–32]. In this Letter, we apply the method of optical control, for the first time, to a high partial wave magnetic Feshbach resonance. We will highlight the universal features in such an optical control. In addition, we will show that interesting situations such as degenerate  $p$ -wave and  $s$ - and  $p$ -wave overlapping resonances can indeed be created.

**Experimental Setup.** Our experiment is performed with  $^{40}\text{K}$  Fermi gas of  $F = 9/2$  manifold with atom number  $N = 2 \times 10^6$  and at temperature  $T/T_F \approx 0.3$ . Details of our setup and state preparations can be found in Ref. [10, 33]. We start with the  $p$ -wave resonance for two atoms in  $|9/2, -7/2\rangle \otimes |9/2, -7/2\rangle$  with a magnetic field along  $\hat{z}$  direction. Because of the magnetic dipolar interaction, the  $m = 0$  resonance occurs at a slightly higher field of 198.8 G and  $m = \pm 1$  resonance at a slightly lower field of 198.3 G, as shown in Fig. 1(b1) and (c1). We first consider the situation that a laser with linear polarization along  $\hat{z}$  is applied to the sample, as shown in Fig. 1(a). Both the rotational and the time reversal symmetry are still preserved, under the condition that the photon recoil energy is sufficiently weak compared to the detuning and can be safely ignored. Hence, the  $m = \pm 1$  resonances remain degenerate even in the presence of the optical control laser.

**Optical Shift of Resonance Position.** When the laser is

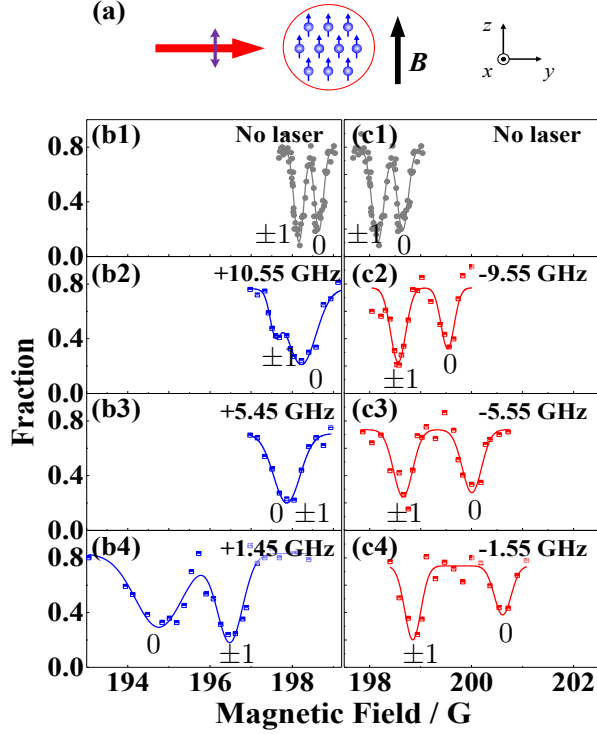


FIG. 1: (Color online) **The  $p$ -wave Feshbach resonance manipulated by a laser field with polarization parallel to the external magnetic field.** (a) Schematic diagram of the laser beam and the external magnetic field. (b) and (c) Atom loss measurements of the  $p$ -wave Feshbach resonance of  $|9/2, -7/2\rangle \otimes |9/2, -7/2\rangle$  (located at 198.3 G for  $m = \pm 1$  and 198.8 G for  $m = 0$  without laser field) as the function of the magnetic field for the different blue (b) and red laser (c) detuning. The laser field drives a bound-to-bound transition around  $\omega_{\text{eg}} \simeq 388104.6$  GHz.

red detuned to the bound-to-bound transition, the energy of the closed channel bound state is effectively pushed down due to the coupling to the excited molecular state. Consequently, it requires larger Zeeman energy to bring the bound state to threshold, and the Feshbach resonance moves toward high magnetic fields. When the laser detuning becomes smaller, the bound state energy experiences stronger level repulsion. As a result, the shift of the resonance position becomes larger. As shown in Fig. 1(c), we find that the position of  $m = 0$  resonance moves much faster than those of the  $m = \pm 1$  resonances as the detuning decreases. For instance, when the red detuning is  $\sim 1.55$  GHz, as shown in Fig. 1(c4), the  $m = \pm 1$  resonance is only shifted to 198.8 G, and the  $m = 0$  resonance is shifted to 201.6 G.

When the laser is blue detuned, the energy of the closed channel molecule is effectively pushed to the higher energy, and it therefore requires less Zeeman energy to bring the molecule to threshold, and consequently the Feshbach resonances move toward low magnetic fields. Similarly,

the resonance of  $m = 0$  moves faster. Hence, for small detuning, the  $m = 0$  resonance locates at a lower field than  $m = \pm 1$  resonance, as shown in Fig. 1(b4). Nevertheless, when the detuning becomes larger, it will eventually recover the situation in absence of the laser field, that is, the  $m = 0$  resonance locates at a higher field than the  $m = \pm 1$  resonance, as shown in Fig. 1(b2). Hence, at an intermediate fine-tuned detuning, the  $m = 0$  resonance will accidentally overlap with the  $m = \pm 1$  resonance, and it creates another interesting situation that all three resonances appear as a single resonance. This is indeed observed as shown in Fig. 1(b3). In another word, this happens when the difference in dipolar interaction energy between molecules is cancelled by the difference in the molecular ac Stark effect. In this accidental situation, it can be viewed as the  $SU(2)$  rotational symmetry is restored

*Experimental Observation of the Universal Feature.* To clearly visualize how the resonance position is shifted by the laser, in Fig. 2 we plot the magnetic field location as a function of the laser detuning. In Fig. 2(a) we consider the  $p$ -wave resonance for spinless  $^{40}\text{K}$  in  $|9/2, -7/2\rangle$  state [24] and the bound-to-bound transition at  $\omega_{\text{eg}} \simeq 388.105$  THz, and in Fig. 2(b) we consider the same  $p$ -wave resonance but a different bound-to-bound transition at  $\omega_{\text{eg}} \simeq 388.31$  THz. In Fig. 2(c) we consider a different  $p$ -wave resonance for spinless  $^{40}\text{K}$  in  $|9/2, -5/2\rangle$  state [34] with the bound-to-bound transition at a similar frequency as Fig. 2(a).

In Fig. 2 we also show that all these cases can be well captured by a simple formula as

$$\mu(B_m - B_{m0}) = -\text{Re} \left[ \frac{I(m)}{\Delta - i\gamma/2} \right], \quad (1)$$

where  $B_m$  and  $B_{m0}$  are the magnetic field position for resonances in presence and in absence of the laser field, respectively,  $\mu$  is the magnetic moment difference between the closed and open channels,  $\Delta$  is the laser detuning from the excited molecular states, and  $\gamma$  is the spontaneous emission rate of excited molecular states.  $I(m)$  represents the laser induced coupling between closed-channel molecule and the excited molecular state. The R.H.S of Eq. (1) is nothing but the laser-induced energy shift of the closed-channel bound state. This formula can be derived from microscopic coupled channel model [35, 36].

By fitting the data shown in Fig. 2 with Eq.(1), we find  $I(0)/I(\pm 1) \approx 2.1, 1.9$  and  $1.9$  for Fig. 2(a-c), respectively. This strongly indicates that  $I(0)/I(\pm 1)$  is a *universal number*. Here *universal* means this ratio is not sensitive to either the choice of closed molecule, that is, which  $p$ -wave resonance to start with (e.g. Fig. 2(a) and (c)), or the choice of the excited molecular state, that is, which bound-to-bound transition to couple to (e.g. Fig. 2(a) and (b)).

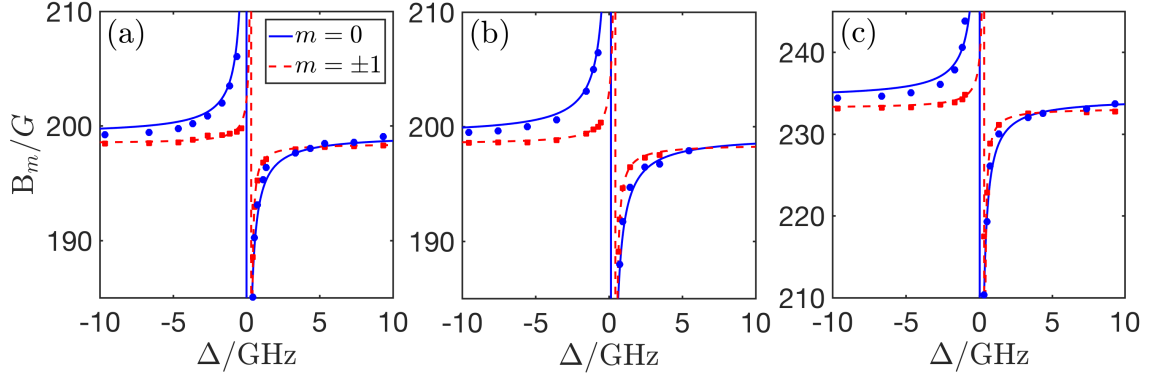


FIG. 2: (Color online) **The position of the shifted Feshbach resonance as a function of the laser detuning.** (a) and (b)  $p$ -wave Feshbach resonance of two atoms in  $|9/2, -7/2\rangle \otimes |9/2, -7/2\rangle$  state [24] at about 198 G with bound-to-bound transition frequency at  $\omega_{eg} \simeq 388.105$  THz (a) and  $\omega_{eg} \simeq 388.31$  THz (b); (c)  $p$ -wave Feshbach resonance of two atoms in  $|9/2, -5/2\rangle \otimes |9/2, -5/2\rangle$  state [34] at about 232 G with bound-to-bound transition frequency at  $\omega_{eg} \simeq 388.105$  THz. The curves are obtained by fitting experimental data by Eq. (1).

*Theoretical Explanation of the Universal Feature.* Here we offer a theoretical explanation why  $I(0)/I(\pm 1)$  is indeed universal. To start with, let us state the necessary quantum numbers to describe a diatomic molecular state in the center-of-mass frame.  $\mathbf{r}_n$  denotes the displacement between two nucleus, and  $\mathbf{r}_{e1}$  and  $\mathbf{r}_{e2}$  are the displacements between two electrons and the center-of-mass. The necessary quantum numbers includes: (i) the total angular momentum  $l$  and its  $\hat{z}$ -component  $m$  (Here  $\hat{x}$ ,  $\hat{y}$  and  $\hat{z}$  label directions in the laboratory frame); (ii) the projection of  $\mathbf{L}_{e1} + \mathbf{L}_{e2}$  along the direction of  $\hat{\mathbf{r}}_n$ , denoted by  $\lambda$ ; (iii)  $n_n$  denoting the vibration between two nucleus, and a set of quantum numbers  $\{n_e\}$  describing the vibration of two electrons; and (iv) the quantum numbers describing the electron and nuclear spin degree of freedom.

For the problem considered here, it is quite reasonable to make following assumptions: (i) The energy splitting between different spin states are much smaller comparing to the laser detuning, such that we can ignore the spin-orbit coupling and the hyperfine coupling, and therefore we will not explicitly include the electron and nuclear spin degree of freedoms. (ii) The energy splitting between states with different quantum number  $l$  are also considered to be small comparing to the laser detuning, and therefore, we treat them as “degenerate” states in the laser coupling. (iii) The radial wave functions of the excited molecular states are not sensitive to the quantum number  $l$  and  $m$ . (ii) and (iii) are essentially based on the consideration that the molecules involved in this process are deeply bound such that their wave function are largely reside in the centrifugal barrier.

Moreover due to the rotational symmetry along  $\hat{z}$ ,  $m$  is a good quantum number between initial and final states. With (i) and (ii), the laser coupling between closed and

excited molecular states is proportional to

$$I(m) \propto \sum_{l^f} |\langle l^f, m, \lambda^f, \{n_e^f\}, n_n^f | \hat{T}_0 | l^i, m, \lambda^i, \{n_e^i\}, n_n^i \rangle|^2, \quad (2)$$

where  $\hat{T}_0$  denotes the  $\hat{z}$ -component of  $\mathbf{r}_{e1} + \mathbf{r}_{e2}$ , and f and i in the upper superscript label the quantum numbers for the initial and final state quantum numbers, respectively. Since we consider a  $p$ -wave resonance, the closed channel molecule should be a  $p$ -wave one, that is,  $l^i = 1$ ; and for two alkali atoms in the electronic ground state ( $\Sigma$ -orbital),  $\lambda^i = 0$ . In the expression for  $I(m)$ , different choice of  $n_n^i$  and  $\{n_e^i\}$  corresponds to different closed channel molecules, and thus, different  $p$ -wave resonance; and different choice of  $n_n^f$  and  $\{n_e^f\}$  corresponds to different excited state molecules, and thus, different bound-to-bound transition frequency.

The key theoretical result is to show that  $I(m)$  can be factorized into

$$I(m) = g(m, \lambda^f) \times h(\{n_e^f\}, n_n^f, \{n_e^i\}, n_n^i, \lambda^f), \quad (3)$$

where  $g$  and  $h$  are two functions. This result follows from (iii) and the use of the Born adiabatic approximation [33]. Thus, we can see that  $I(0)/I(\pm 1)$  only depends on  $\lambda^f$  and

$$\frac{I(0)}{I(\pm 1)} = \begin{cases} 3 & \text{for } \lambda^f = 0, \\ 1/2 & \text{for } \lambda^f = \pm 1. \end{cases} \quad (4)$$

$I(0)/I(\pm 1)$  is independent of  $n_n^f$ ,  $\{n_e^f\}$ ,  $n_n^i$  and  $\{n_e^i\}$ , that is to say, is independent on the choice of  $p$ -wave resonance, and up to these two different values, is independent of the choice of the bound-to-bound transition.

This result provides a qualitative explanation of the experimental observations. Assuming the three cases shown in Fig. 2 all come from excited molecular states with  $\lambda^f = 0$ , it is consistent with that fact that the  $m = 0$  resonance always moves faster than  $m = \pm 1$  resonance, and

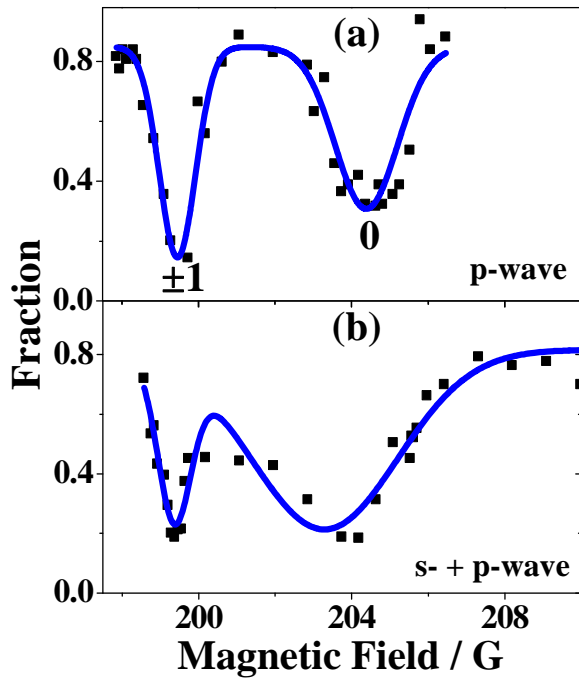


FIG. 3: (Color online) **The p-wave Feshbach resonance overlapping with s-wave resonance by the laser field..** (a) Loss measurements of the p-wave Feshbach resonance of  $|9/2, -7/2\rangle \otimes |9/2, -7/2\rangle$  as the function of the magnetic field for the red laser detuning. (b) Loss measurements of the p- and s-wave Feshbach resonances of  $|9/2, -7/2\rangle \otimes |9/2, -9/2\rangle$  as the function of the magnetic field for the red laser detuning. The laser beam propagating along the  $\hat{y}$  axis, is linearly polarized parallel to external magnetic field and red detuning with 1.1 GHz.

the ratio  $I(0)/I(\pm 1)$  is nearly a constant. The quantitative difference between our theoretical and experimental results is likely due to the assumptions (i)-(iii) are not perfectly obeyed in practices.

**Overlapping s- and p-wave Resonance.** Recently, several works have predicted that interesting many-body physics can occur when a p-wave Feshbach resonance sits nearby an s-wave one [37–40]. For instance, it has been predicted that for a one-dimensional Fermi gas with strong s-wave interaction, an extra p-wave interaction can make the system favor an itinerant ferromagnetic phase [39, 40], providing a new mechanism for itinerant ferromagnetism; and it has also been predicted that interacting pairing structure can happen for a three-dimensional Fermi gas with overlapping s- and p-wave resonances. Nevertheless, without the optical control, even through in  $^{40}\text{K}$  the s- and p-wave resonances are quite close, the p-wave resonances sitting at 198.3 G and 198.8 G are barely within the range (8 G) of the s-wave resonance sitting at 201.6 G [41].

With our optical control, as shown in Fig. 3, for red detuning 1.1 GHz, one of the resonance with  $m = 0$  can be shifted by about 10 G in practice, and therefore overlaps

with the s-wave resonance. Fig 3 (a) shows the loss for single component Fermi gas with only  $|9/2, -7/2\rangle$  state and with applied optical control, and Fig. 3(b) shows the loss feature for a mixture of  $|9/2, -7/2\rangle$  and  $|9/2, -9/2\rangle$ . One can see that one of the p-wave resonance is entirely buried inside the s-wave resonance. Therefore it creates the situation where the predications from Ref. [37–40] can be tested in this system.

**Conclusion.** In summary, we have studied the optical control of a p-wave Feshbach resonance by utilizing bound-to-bound transitions driven by a laser field. The main finding is a universal feature of this optical control, that is, the ratio  $I(0)/I(\pm 1)$  to large extent is a universal constant. By this optical control, we demonstrate that intriguing scenarios can happen such as a p-wave resonance can overlap with an s-wave resonance. We have also considered the situation that the polarization of the laser is not along  $\hat{z}$  but in the  $xy$  plane. This breaks the rotational symmetry and all three resonances will split. This allows us to access independent control of all three resonances [33]. Our work opens many opportunities for investigating interesting few- and many-body problems in these settings.

**Acknowledgment.** This work is supported by MOST under Grant No. 2016YFA0301600 and No. 2016YFA0301602, NSFC Grant No. 11234008, No. 11474188, No. 11704234, No. 11325418, No. 11734010, No. 11434011, No. 11674393, the Fund for Shanxi "1331 Project" Key Subjects Construction, the Fundamental Research Funds for the Central Universities, and the Research Funds of Renmin University of China under Grant No.16XNLQ03, 17XNH054.

\* They contribute equally to this work.

† Correspondence may be addressed to Lianghai Huang (huanglh06@126.com).

‡ Correspondence may be addressed to Jing Zhang (jzhang74@yahoo.com, jzhang74@sxu.edu.cn).

- [1] C. Chin, R. Grimm, P. Julienne, and E. Tiesinga, Rev. Mod. Phys. **82**, 1225 (2010).
- [2] P. O. Fedichev, Yu. Kagan, G. V. Shlyapnikov, and J. T. M. Walraven, Phys. Rev. Lett. **77**, 2913 (1996).
- [3] R. Yamazaki, S. Taie, S. Sugawa, and Y. Takahashi, Phys. Rev. Lett. **105**, 050405 (2010).
- [4] R. Qi and H. Zhai, Phys. Rev. Lett. **106**, 163201 (2011).
- [5] P. Zhang, P. Naidon, and M. Ueda, Phys. Rev. Lett. **103**, 133202 (2009).
- [6] D. M. Bauer, M. Lettner, C. Vo, G. Rempe, and S. Durr, Nature Phys. **5**, 339 (2009).
- [7] D. M. Bauer, M. Lettner, C. Vo, G. Rempe, and S. Durr, Phys. Rev. A **79**, 062713 (2009).
- [8] G. Thalhammer, M. Theis, K. Winkler, R. Grimm, and J. H. Denschlag, Phys. Rev. A **71**, 033403 (2005).
- [9] H. Wu and J. E. Thomas, Phys. Rev. Lett. **108**, 010401 (2012).
- [10] Z. Fu, P. Wang, L. Huang, Z. Meng, H. Hu, and J. Zhang,

- Phys. Rev. A **88**, 041601 (2013).
- [11] L. W. Clark, L.-C. Ha, C.-Y. Xu, and C. Chin, Phys. Rev. Lett. **115**, 155301 (2015).
  - [12] A. Jagannathan, N. Arunkumar, J. A. Joseph, and J.E. Thomas, Phys. Rev. Lett. **116**, 075301 (2016)
  - [13] Y. Zhang, W. Liu, and H. Hu, Phys. Rev. A **90**, 052722 (2014).
  - [14] J. Jie and P. Zhang, Phys. Rev. A **95** 060701 (2017).
  - [15] N. Read and D. Green, Phys. Rev. B **61**, 10267(2000)
  - [16] T.-L. Ho and R. B. Diener, Phys. Rev. Lett. **94**, 090402 (2005)
  - [17] Z. Yu, J. H. Thywissen, S. Zhang, Phys. Rev. Lett. **115**, 135304 (2015); Phys. Rev. Lett. **117**, 019901 (2016).
  - [18] S. M. Yoshida and M. Ueda, Phys. Rev. Lett. **115**, 135303 (2015)
  - [19] C. Luciuk, S. Trotzky, S. Smale, Z. Yu, S. Zhang, J. H. Thywissen, Nat. Phys. **12**, 599 (2016).
  - [20] X. Cui, Phys. Rev. A **95**, 030701(R) (2017).
  - [21] A. Kitaev, Phys. Usp. **44**, 131 (2001)
  - [22] V. Gurarie, L. Radzihovsky, and A.V. Andreev, Phys. Rev. Lett. **94**, 230403 (2005)
  - [23] C.-H. Cheng and S.-K. Yip, Phys. Rev. Lett. **95**, 070404 (2005).
  - [24] C. A. Regal, C. Ticknor, J. L. Bohn, and D. S. Jin, Phys. Rev. Lett. **90**, 053201 (2003).
  - [25] C. Ticknor, C. A. Regal, D. S. Jin and J. L. Bohn, Phys. Rev. A **69**, 042712 (2004).
  - [26] J. Zhang, E. G. M. van Kempen, T. Bourdel, L. Khaykovich, J. Cubizolles, F. Chevy, M. Teichmann, L. Tarruell, S. J. J. M. F. Kokkelmans, and C. Salomon, Phys. Rev. A **70**, 030702 (2004).
  - [27] K. Günter, T. Stöferle, H. Moritz, M. Köhl, and T. Esslinger, Phys. Rev. Lett. **95**, 230401 (2005).
  - [28] C. H. Schunck, M. W. Zwierlein, C. A. Stan, S. M. F. Raupach, W. Ketterle, A. Simoni, E. Tiesinga, C. J. Williams, and P. S. Julienne, Phys. Rev. A **71**, 045601 (2005).
  - [29] J. P. Gaebler, J. T. Stewart, J. L. Bohn, and D. S. Jin, Phys. Rev. Lett. **98**, 200403 (2007).
  - [30] J. Fuchs, C. Ticknor, P. Dyke, G. Veeravalli, E. Kuhnle, W. Rowlands, P. Hannaford, and C. J. Vale, Phys. Rev. A **77**, 053616 (2008).
  - [31] Y. Inada, M. Horikoshi, S. Nakajima, M. Kuwata-Gonokami, M. Ueda, and T. Mukaiyama, Phys. Rev. Lett. **101**, 100401 (2008).
  - [32] T. Nakasuji, J. Yoshida, and T. Mukaiyama, Phys. Rev. A **88** 012710 (2013).
  - [33] See the supplementary material for: (i) details of experimental setup; (ii) proof of Eq.(3) and Eq.(4); (iii) various laser polarization.
  - [34] A. Ludewig, *Feshbach resonance in  $^{40}\text{K}$* , University of Amsterdam, 2012.
  - [35] P. Zhang, P. Naidon and M. Ueda, Phys. Rev. A **82**, 062712 (2010).
  - [36] T. Köhler, K. Góral and P. S. Julienne, Rev. Mod. Phys., **78**, 1311 (2006).
  - [37] L. Zhou, W. Yi, X. Cui, arXiv:1512.09313.
  - [38] F. Qin, X. Cui, and W. Yi, Phys. Rev. A **94**, 063616 (2016).
  - [39] L. Yang, X. Guan and X. Cui, Phys. Rev. A **93**, 051605(R) (2016).
  - [40] Y. Jiang, D. V. Kurllov, X.-W. Guan, F. Schreck, and G. V. Shlyapnikov, Phys. Rev. A **94**, 011601(R) (2016).
  - [41] T. Loftus, C. A. Regal, C. Ticknor, J. L. Bohn, and D. S. Jin, Phys. Rev. Lett. **88**, 173201 (2002).

# Supplementary for “Universal Feature in Optical Control of a $p$ -wave Feshbach Resonance”

## EXPERIMENTAL SETUP

We perform our experiments by employing a fermionic gas of  $^{40}\text{K}$  atoms of the  $F = 9/2$  manifold. The experiment starts with a Fermi gas of  $|9/2, 9/2\rangle$  with atom number  $N = 2 \times 10^6$  and at a temperature of  $T/T_F \approx 0.3$  in a crossed 1064 nm optical dipole trap.  $T_F$  is the Fermi temperature defined as  $T_F = (6N)^{1/3} \hbar \bar{\omega} / k_B$  with  $\bar{\omega} \simeq 2\pi \times 80$  Hz labels the geometric trapping frequency. The fermionic atoms are transferred to  $|9/2, -9/2\rangle$  state as the initial state via a rapid adiabatic passage induced by a RF field at 5 G. Then, the Fermi gas is transferred to the  $|9/2, -7/2\rangle$  state using a RF field with duration of 30 ms at  $B \simeq 219.4$  G, where the frequency of center is 47.45 MHz and the width is 0.3 MHz. In addition to these, we can also prepare the Fermi gases at the  $|9/2, -5/2\rangle$  state via transferring atoms in  $|9/2, -7/2\rangle$  state to the  $|9/2, -5/2\rangle$  state by a RF field of  $\pi$  pulse.

Subsequently, a homogeneous magnetic bias field  $B_{\text{exp}}$  is applied in the  $\hat{z}$  axis (gravity direction) produced by quadrupole coils, which is operating in the Helmholtz configuration. Two laser beams propagating along  $\hat{y}$  and  $\hat{z}$  respectively are used as the tools to manipulate the  $p$ -wave Feshbach resonance and are extracted from a continuous-wave Ti-sapphire single frequency laser and focused at the position of the atomic cloud with  $1/e^2$  radii of 200  $\mu\text{m}$ , larger than the size of the degenerate Fermi gas. The laser beams is frequency-shifted by an acousto-optic modulators (AOM), which allows precise control of the laser intensity and duration time of the pulse.

In order to control and observe the  $p$ -wave Feshbach resonance, we start with the ultracold Fermi gases in the  $|9/2, -7/2\rangle$  state at  $B \simeq 219.4$  G. Then we adiabatically ramp the magnetic-field to the various expected field  $B_{\text{exp}}$  during 1 ms, and hold 20 ms to observe the atomic losses at  $|9/2, -7/2\rangle$  state by counting the number of atoms. Subsequently, the laser is switched on and couples the closed channel molecular state to the excited molecular states as shown in Fig. 1(a). Finally, we immediately turn off laser beam, the optical trap, and the magnetic field, and let the atoms ballistically expand in 12 ms and take the time-of-flight (TOF) absorption image. The number of atoms in  $|9/2, -7/2\rangle$  state is obtained from the TOF image.

## BOUND-TO-BOUND SPECTROSCOPY

We first measure the bound-to-bound spectroscopy for excited  $^{40}\text{K}_2$  molecules below the  $^2P_{1/2} + ^2S_{1/2}$  threshold near  $p$ -wave Feshbach resonance. The magnetic-field  $B_{\text{exp}}$  is set to 198.3 G. At this value the atoms are subject to inelastic loss since the energy of the closed channel molecular state  $m = \pm 1$  coincides with the energy of two free atoms. When the laser illuminates atomic gas and is near resonant with a bound-to-bound transition from  $\phi_g$  to one of the excited molecular states  $\phi_e$ , a shift of the resonance position is induced by ac-stark effect and the peak location of atomic losses are shifted. Fig. 1(b) shows the bound-to-bound spectroscopy near  $p$ -wave Feshbach resonance. Here, the laser intensity is  $I = 60$  mW and the laser wavelength ranges from 771.5 nm to 772.7 nm. We compare this bound-to-bound spectroscopy near  $p$ -wave Feshbach resonance with that near  $s$ -wave Feshbach resonance of  $|9/2, -9/2\rangle \otimes |9/2, -7/2\rangle$  at the magnetic field  $B = 201.6$  G as shown in Fig. 1(c). This bound-to-bound spectroscopy near  $s$ -wave Feshbach resonance was reported in our earlier work [1], in which Feshbach molecules are prepared below the resonance at  $B = 201.6$  G and its losses are measured during the laser drive the bound-to-bound transition. The bound-to-bound spectroscopy obtained by two different ways show highly consistency. The observed peaks in the bound-to-bound spectroscopy near  $p$ -wave Feshbach resonance correspond to the vibrational level of the excited molecular states. There should be the multi-substructures at each vibrational level induced by vibration, rotation, hyperfine interaction, and Zeeman interaction of molecules, which were observed in the bound-to-bound spectroscopy near  $s$ -wave Feshbach resonance in our earlier work [1].

## PROOF OF EQS. (3) AND (4)

Now we prove Eq. (3) and Eq. (4) in the main text by calculate the intensity  $I(m)$  of the laser-induced coupling between the closed-channel bound state and the excited molecular state.

We start with a brief introduction of the wave function of the molecular state  $|l, m, \lambda, n_n, \{n_e\}\rangle$ . Since the freedom of the inner shell electron can be safely ignored, a homonuclear diatomic molecule, *e.g.*, a molecule of two  $^{40}\text{K}$  atoms



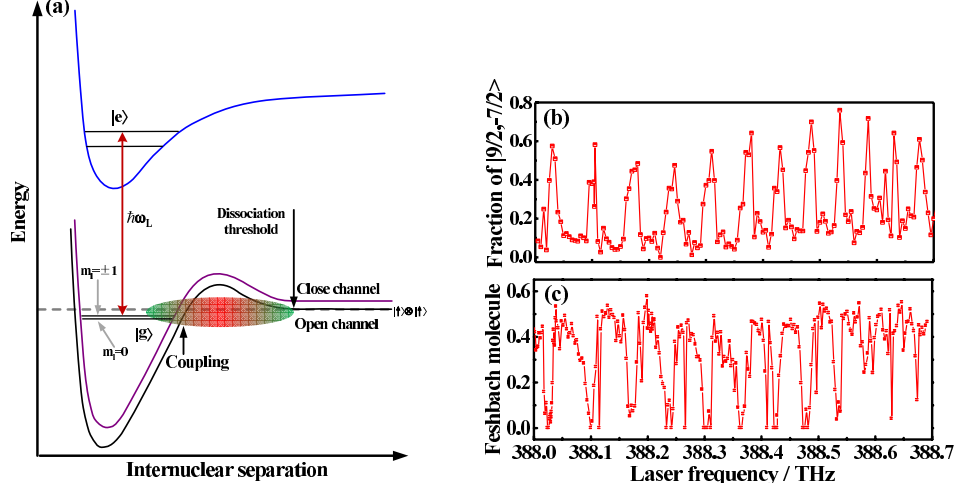


FIG. 1: (Color online) **Energy level diagram and excited molecule state spectroscopy.** (a) Schematic diagram of the energy curves of two atoms. Bound-to-bound transition from closed channel molecular state  $\phi_g$  to one of the excited molecular states  $\phi_e$  occurs when a near resonant laser with frequency  $\omega_L$  is applied. Two curves at the low energy end denotes the energy of two single-component  $^{40}\text{K}$  atoms in electronic ground state. The curve at high energy end denote the energy of two atoms composed by one electronic ground state atom and one electronic excited state atom. (b) Bound-to-bound spectroscopy below the  $^2P_{1/2} + ^2S_{1/2}$  threshold near  $p$ -wave Feshbach resonance of  $|9/2, -7/2\rangle \otimes |9/2, -7/2\rangle$  at the magnetic field  $B = 198.3$  G. (c) Bound-to-bound spectroscopy below the  $^2P_{1/2} + ^2S_{1/2}$  threshold near  $s$ -wave Feshbach resonance of  $|9/2, -9/2\rangle \otimes |9/2, -7/2\rangle$  at the magnetic field  $B = 201.6$  G.

can be viewed as being composed by two nuclei  $n_{1,2}$  and two outermost shell electrons  $e_{1,2}$  (Fig. 2). We study the relative motion of these four particles, which is decoupled from the center-of-mass motion. Thus, as shown in Fig. 2, we choose the origin of our coordinate system to be the center-of-mass position, which is approximated as the middle point of the two nuclei. We also define the  $x$ -,  $y$ - and  $z$ -axes to be parallel to the ones of the lab frame. In our system the molecule wave function is a function of the relative position  $\mathbf{r}_n$  of the two nuclei and the position  $\mathbf{r}_{e_{1,2}}$  of the electrons  $e_{1,2}$  (Fig. 2). Notice that  $\mathbf{r}_{e_i}$  ( $i = 1, 2$ ) is actually the relative position of  $e_i$  and the center of mass of the two nuclei. As shown in the main text, spin-orbit coupling and hyperfine interaction are ignored. Thus in our calculation we only consider the spatial motion of the electrons and nuclei.

In our system, the total orbital angular momentum of all the four particles is denoted by  $\mathbf{L}$ , and the orbital angular momentum of the electron  $e_i$  ( $i = 1, 2$ ) is denoted by  $\mathbf{L}_{e_i}$ . For simplicity, we ignore the fine and hyperfine interaction and only consider the Coulomb interaction. Therefore, for our system the total angular momentum  $\mathbf{L}$  and the component of  $\mathbf{L}_{e_1} + \mathbf{L}_{e_2}$  in the direction of  $\mathbf{r}_n$  are conserved. Thus, the molecule state can be denoted as  $|l, m, \lambda, n_n, \{n_e\}\rangle$ , where  $l$  and  $m$  are the quantum numbers for  $\mathbf{L}^2$  and the  $z$ -component of  $\mathbf{L}$ , respectively,  $\lambda$  is the quantum number for the component of  $\mathbf{L}_{e_1} + \mathbf{L}_{e_2}$  along the direction of  $\mathbf{r}_n$ , while  $n_n$  and  $\{n_e\}$  are the nuclear and the electronic vibrational quantum numbers, respectively. Under the Born adiabatic approximation [2], the molecular wave function

$$\Psi_{l,m,\lambda,n_n,\{n_e\}}(\mathbf{r}_n; \mathbf{r}_{e_1}, \mathbf{r}_{e_2}) \equiv \langle \mathbf{r}_n; \mathbf{r}_{e_1}, \mathbf{r}_{e_2} | l, m, \lambda, n_n, \{n_e\} \rangle \quad (1)$$

can be factorized as

$$\Psi_{l,m,\lambda,n_n,\{n_e\}}(\mathbf{r}_n; \mathbf{r}_{e_1}, \mathbf{r}_{e_2}) = \psi_{l,m,\lambda,n_n,\{n_e\}}^{(n)}(\mathbf{r}_n) \psi_{\{n_e\},\lambda}^{(e)}(\mathbf{r}_n; \mathbf{r}_{e_1}, \mathbf{r}_{e_2}). \quad (2)$$

Here  $\psi_{\{n_e\},\lambda}^{(e)}$  is the wave function of the two outermost shell electrons when the positions of the two nuclei are pinned down, and can be expressed as

$$\psi_{\{n_e\},\lambda}^{(e)}(\mathbf{r}_n; \mathbf{r}_{e_1}, \mathbf{r}_{e_2}) = e^{-i\hat{L}_z^{(e)}\phi} e^{-i\hat{L}_y^{(e)}\theta} \phi_{\{n_e\},\lambda}(r_n; \mathbf{r}_{e_1}, \mathbf{r}_{e_2}), \quad (3)$$

where  $r_n$ ,  $\theta$  and  $\phi$  are the norm, polar angle and azimuthal angle of  $\mathbf{r}_n$ , respectively (Fig. 2),  $\hat{L}_\alpha^{(e)}$  ( $\alpha = x, y, z$ ) is the component of  $\mathbf{L}_{e_1} + \mathbf{L}_{e_2}$  along the  $\alpha$ -axis, and  $\phi_{\{n_e\},\lambda}$  is the electronic wave function when the nuclei are pinned on

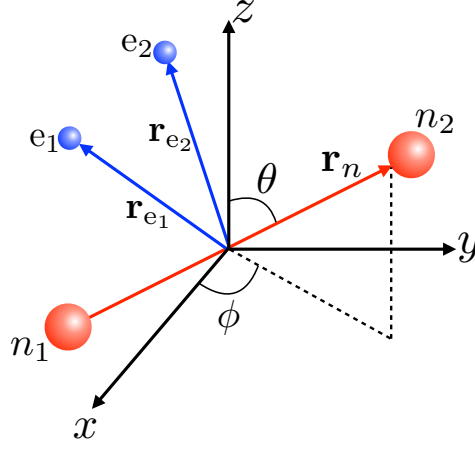


FIG. 2: (Color online) The coordinate system used in our calculation.

the  $z$ -axis, which satisfies  $\hat{L}_z^{(e)} \phi_{\{n_e\}, \lambda}(r_n; \mathbf{r}_{e1}, \mathbf{r}_{e2}) = \lambda \phi_{\{n_e\}, \lambda}(r_n; \mathbf{r}_{e1}, \mathbf{r}_{e2})$ . Moreover, it can be shown that the nuclear wave function  $\psi_{l, m, \lambda, n_n, \{n_e\}}(\mathbf{r}_n)$  can be further factorized as [3]

$$\psi_{l, m, \lambda, n_n, \{n_e\}}(\mathbf{r}_n) = \chi_{l, m, \lambda, n_n, \{n_e\}}(r_n) \sqrt{\frac{2l+1}{4\pi}} D_{\lambda, m}^{(l)}(\phi, \theta, 0), \quad (4)$$

with  $D_{\lambda, m}^{(l)}(\alpha, \beta, \gamma)$  being the Wigner's  $D$ -function and  $\chi_{l, m, \lambda, n_n, \{n_e\}}(r_n)$  being the radial wave function of the nuclei.

With the above results we can calculate the dipole transition matrix element  $\langle l^f, m, \lambda^f, n_n^f, \{n_e^f\} | \hat{T}_0 | l^i, m, \lambda^i, n_n^i, \{n_e^i\} \rangle$ , which appears in Eq. (2) of the main text. This matrix element can be expressed as

$$\begin{aligned} & \langle l^f, m, \lambda^f, n_n^f, \{n_e^f\} | \hat{T}_0 | l^i, m, \lambda^i, n_n^i, \{n_e^i\} \rangle \\ &= \int d\mathbf{r}_{e1} d\mathbf{r}_{e2} d\mathbf{r}_n \left[ \Psi_{l^f, m, \lambda^f, n_n^f, \{n_e^f\}}^*(\mathbf{r}_n; \mathbf{r}_{e1}, \mathbf{r}_{e2}) \hat{T}_0 \Psi_{l^i, m, \lambda^i, n_n^i, \{n_e^i\}}(\mathbf{r}_n; \mathbf{r}_{e1}, \mathbf{r}_{e2}) \right], \end{aligned} \quad (5)$$

where

$$\hat{T}_0 = (z_{e1} + z_{e2}), \quad (6)$$

with  $z_{ei}$  ( $i = 1, 2$ ) is the  $z$ -component of  $\mathbf{r}_{ei}$ . For future use, we further define the operators

$$\hat{T}_{\pm 1} = \left[ \frac{\mp(x_{e1} + x_{e2}) - i(y_{e1} + y_{e2})}{\sqrt{2}} \right], \quad (7)$$

with  $x_{ei}$  and  $y_{ei}$  ( $i = 1, 2$ ) being the  $x$ - and  $y$ -component of  $\mathbf{r}_{ei}$ , respectively. It is clear that  $\hat{T}_j$  ( $j = 0, \pm 1$ ) form rank-1 irreducible tensor operators under the total rotation of the two electrons, and thus satisfy

$$e^{i\hat{L}_y^{(e)}\theta} e^{i\hat{L}_z^{(e)}\phi} \hat{T}_0 e^{-i\hat{L}_z^{(e)}\phi} e^{-i\hat{L}_y^{(e)}\theta} = \sum_{q'=0, \pm 1} \hat{T}_{q'} D_{q', 0}^{(1)}(\phi, \theta, 0). \quad (8)$$

Substituting Eqs.(3,4) into Eq.(2) and then into Eq.(5), and using Eq. (8) and the facts that  $l^i = 1$  and  $\lambda^i = 0$ , we obtain

$$\langle l^f, m, \lambda^f, n_n^f, \{n_e^f\} | \hat{T}_0 | l^i, m, \lambda^i, n_n^i, \{n_e^i\} \rangle = (-1)^{\lambda^f - m} \sqrt{3(2l^f + 1)} A_{\{n_e^f\}, n_n^f, \{n_e^i\}, n_n^i, l^f, m, \lambda^f} \begin{pmatrix} l^f & 1 & 1 \\ -\lambda^f & \lambda^f & 0 \end{pmatrix} \begin{pmatrix} l^f & 1 & 1 \\ -m & 0 & m \end{pmatrix}, \quad (9)$$

where  $\begin{pmatrix} j_1 & j_2 & j_3 \\ m_1 & m_2 & m_3 \end{pmatrix}$  is the Winger-3j symbols and  $A_{\{n_e^f\}, n_n^f, \{n_e^i\}, n_n^i, l^f, m, \lambda^f}$  is defined as

$$\begin{aligned} & A_{\{n_e^f\}, n_n^f, \{n_e^i\}, n_n^i, l^f, m, \lambda^f} = \\ & \int_0^\infty dr_n \left\{ r_n^2 \chi_{l^f, m, \lambda^f, \{n_e^f\}, n_n^f}^*(r_n) \chi_{l^i=1, m, \lambda^i=0, \{n_e^i\}, n_n^i}(r_n) \int d\mathbf{r}_{e1} d\mathbf{r}_{e2} \left[ \phi_{\{n_e^f\}, \lambda^f}^*(r_n; \mathbf{r}_{e1}, \mathbf{r}_{e2}) \hat{T}_{\lambda^f} \phi_{\{n_e^i\}, \lambda^i=0}(r_n; \mathbf{r}_{e1}, \mathbf{r}_{e2}) \right] \right\}. \end{aligned} \quad (10)$$



In the derivation of Eq. (9), the relations that  $D_{m'm}^{(l)}(\phi, \theta, 0)^* = (-1)^{m'-m} D_{-m', -m}^{(l)}(\phi, \theta, 0)$  and

$$\int \frac{\sin \phi d\phi d\theta}{4\pi} D_{m'_1 m_1}^{(j_1)}(\phi, \theta, 0) D_{m'_2 m_2}^{(j_2)}(\phi, \theta, 0) D_{m'_3 m_3}^{(j_3)}(\phi, \theta, 0) = \begin{pmatrix} j_1 & j_2 & j_3 \\ m'_1 & m'_2 & m'_3 \end{pmatrix} \begin{pmatrix} j_1 & j_2 & j_3 \\ m_1 & m_2 & m_3 \end{pmatrix}. \quad (11)$$

are adopted[3].

Now we consider the dependence of  $A_{\{n_e^f\}, n_n^f, \{n_e^i\}, n_n^i, l^f, m, \lambda^f}$  on the quantum numbers  $l^f$  and  $m$  of the final state. In the radial Schrödinger equation satisfied by  $\chi_{\{n_e^f\}, n_n^f, l^f, m, \lambda^f}(r_n)$ , the value of  $l^f$  and  $m$  only influence the intensity of the centrifugal potential which is proportional to  $-r_n^{-2}$ , and thus do not have strong effects for the deep bound state. As shown in the main text, here we assume that the excited molecular states are deep bound states and thus assume the radial wave function  $\chi_{\{n_e^f\}, n_n^f, l^f, m, \lambda^f}(r_n)$  to be approximately independent of the values of  $l^f$  and  $m$ . Therefore, according to Eq. (10), the parameter  $A_{\{n_e^f\}, n_n^f, \{n_e^i\}, n_n^i, l^f, m, \lambda^f}$  is also independent of  $l^f$  and  $m$ . Therefore, we can simplify the notation

$$A_{\{n_e^f\}, n_n^f, \{n_e^i\}, n_n^i, l^f, m, \lambda^f} \rightarrow A_{\{n_e^f\}, n_n^f, \{n_e^i\}, n_n^i, \lambda^f}, \quad (12)$$

and rewrite Eq. (9) in a more concise form as

$$\langle l^f, m, \lambda^f, n_n^f, \{n_e^f\} | \hat{T}_0 | l^i, m, \lambda^i, n_n^i, \{n_e^i\} \rangle = (-1)^{\lambda^f - m} \sqrt{3(2l^f + 1)} A_{\{n_e^f\}, n_n^f, \{n_e^i\}, n_n^i, \lambda^f} \begin{pmatrix} l^f & 1 & 1 \\ -\lambda^f & \lambda^f & 0 \end{pmatrix} \begin{pmatrix} l^f & 1 & 1 \\ -m & 0 & m \end{pmatrix}. \quad (13)$$

Eq. (13) shows that the dependence of  $\langle l^f, m, \lambda^f, \{n_e^f\}, n_n^f | \hat{T}_0 | l^i, m, \lambda^i, \{n_e^i\}, n_n^i \rangle$  on  $l^f$  and  $m$  are all included in the Wigner-3j symbols and the factor  $\sqrt{3(2l^f + 1)}$ , and thus can be evaluated precisely.

Substituting Eq. (13) into Eq. (2) of the main text, we immediately obtain the laser coupling intensity  $I(m)$ :

$$I(m) = g(m, \lambda^f) \times h(\{n_e^f\}, n_n^f, \{n_e^i\}, n_n^i, \lambda^f), \quad (14)$$

where

$$g(m, \lambda^f) = \sum_{l^f} 3(2l^f + 1) \begin{pmatrix} l^f & 1 & 1 \\ -\lambda^f & \lambda^f & 0 \end{pmatrix}^2 \begin{pmatrix} l^f & 1 & 1 \\ -m & 0 & m \end{pmatrix}^2, \quad (15)$$

and

$$h(\{n_e^f\}, n_n^f, \{n_e^i\}, n_n^i, \lambda^f) = |A_{\{n_e^f\}, n_n^f, \{n_e^i\}, n_n^i, \lambda^f}|^2. \quad (16)$$

Eq. (14) is just Eq.(3) of our main text.

Furthermore, using Eqs. (14-16) we can immediately obtain the result  $I(+1) = I(-1)$ , as well as Eq. (4) of our main text:

$$\frac{I(0)}{I(\pm 1)} = \begin{cases} 3, & \text{for } \lambda^f = 0 \\ 1/2, & \text{for } \lambda^f = \pm 1 \end{cases}. \quad (17)$$

Notice that this result is independent of the value of  $\{n_e^f\}$ . This result means that if the  $\pi$ -polarized laser couples the closed-channel bound state of the magnetic Feshbach resonance to the excited molecular states with  $\lambda^f = 0$  (i.e., the states in the electronic  $\Sigma$ -orbit), then the shift of the resonance point for  $m = 0$  is more significant than that for  $m = \pm 1$ . On the other hand, if the excited molecular states have  $\lambda^f = \pm 1$  (i.e., the states are in the electronic  $\Pi$ -orbit), then the shift of the resonance point for  $m = \pm 1$  is more significant than that for  $m = 0$ . This result implies in all of our experiments the laser induce the coupling to the excited molecule states with  $\lambda^f = 0$ .

### VARYING LASER POLARIZATIONS.

We also consider the situation where the laser polarization is changed. In Fig. 3 we show the case where the laser propagates along  $\hat{y}$  and the polarization is along  $\hat{x}$ . In this case the laser breaks rotational symmetry along  $\hat{z}$  and the  $m = \pm 1$  resonances split as a result. We find that when the laser is red detuned and large in strength, one of the peaks from  $m = \pm 1$  manifold moves closer to  $m = 0$  resonance and they become incidentally degenerate, as shown in

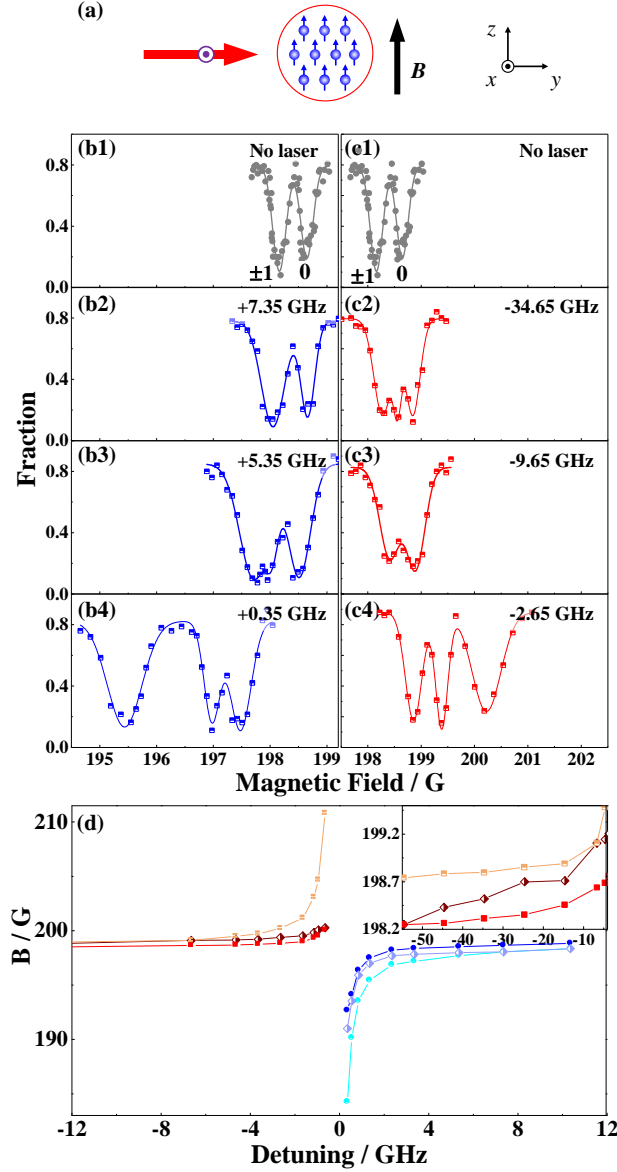


FIG. 3: (Color online) **The  $p$ -wave Feshbach resonance manipulated by the laser field with the polarization perpendicular to external magnetic field.** (a) Schematic diagram of the laser beam and the external magnetic field. The laser beam propagating along the  $\hat{y}$  axis, is linearly polarized perpendicular to external magnetic field. (b) and (c) Atom loss measurements of the  $p$ -wave Feshbach resonance of  $|9/2, -7/2\rangle \otimes |9/2, -7/2\rangle$  as the function of the magnetic field for the different blue and red laser detuning. (d) The resonance position of the shifted Feshbach resonance as a function of the laser detuning. Three different lines correspond to the  $m = 0$  and  $m = \pm 1$  resonances respectively.

Fig. 3(c3). When the laser frequency is tuned further to the resonance, the  $m = 0$  peak moves much more quickly, still consistent with the analysis in main text.

In Fig. 4 we show a different case in which the laser propagates along the magnetic field direction but the polarization is circularly polarized in the plane perpendicular to the magnetic field. Here we fix the laser detuning at  $-2.6$  GHz and find that the resonance position behaves differently depending on the laser ellipticity  $\xi$ . ( $\xi = 0$  denote linear polarization, and  $\xi = \pm$  denotes left and right circular polarization.) Thus, we see that by combining laser detuning and ellipticity, one can almost independently control all three resonances.

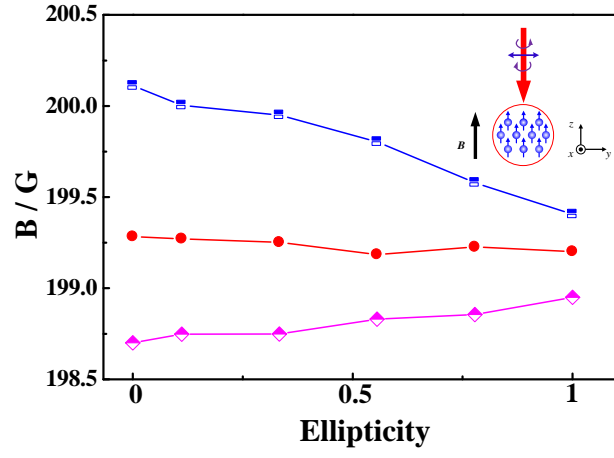


FIG. 4: (Color online) **The p-wave Feshbach resonance manipulated by the laser field propagating along the external magnetic field with circular polarization.** The position of the shifted Feshbach resonance as a function of the ellipticity. Here, laser detuning is  $-2.6$  GHz. Inset: Schematic diagram of the laser beam and the external magnetic field. Three different lines correspond to the  $m = 0$  and  $m = \pm 1$  resonances respectively.

- 
- [1] Z. Fu, P. Wang, L. Huang, Z. Meng, H. Hu, and J. Zhang, Phys. Rev. A **88**, 041601 (2013).
  - [2] J. Brown and A. Carrington, *Rotational Spectroscopy of Diatomic Molecules*, Cambridge University Press, 2003.
  - [3] L. D. Landau and E. M. Lifshitz, *Quantum Mechanics: Non Realistic Theory*, Third edition, Pergamon Press.